atoms

MDPI

Article

Channeling of Protons through Radial Deformed Double Wall Carbon Nanotubes

Duško Borka * and Vesna Borka Jovanović

Atomic Physics Laboratory (040), Vinča Institute of Nuclear Sciences, University of Belgrade, P.O. Box 522, 11001 Belgrade, Serbia

* Correspondence: dusborka@vinca.rs; Tel.: +381-11-630-8425

Received: 10 July 2019; Accepted: 5 September 2019; Published: 7 September 2019

Abstract: In this study we presented a theoretical investigation of the channeling of high energy protons with the radial deformed (10, 0)@(5, 0) double-wall carbon nanotubes (DWNTs). Proton energy is varied from 0.1 to 10 GeV. The channeling potential within the deformed DWNTs is presented. A Monte Carlo (MC) simulation is used to obtain spatial and angular distributions of channeled protons with radially deformed DWNTs. We treated problem relativistically. This is the first time that we presented spatial and angular distributions of channeled protons with radially deformed DWNTs. Our results show that the spatial and angular distributions depend strongly of nanotube lengths, proton energy, and especially of level of radial deformation of nanotube. Multi-wall nanotubes (MWNTs) can be technically realised with better channeling performance then single-wall nanotubes (SWNTs) and that is why we believe that these results may be useful for production and guiding of nanosized ion beams.

Keywords: double wall carbon nanotubes; channeling; radial deformation

1. Introduction

After the discovery of the carbon nanotubes in 1991 [1], a lot of theoretical groups started to work on theoretical modeling and computer simulation of ion channeling through carbon nanotubes [2–29].

Klimov and Letokhov [2] predicted that carbon nanotubes could be used to channel positively charged particles. They modeled ion channeling in GeV energy range. Detailed study about the influence of the nanotube diameter on the channeling high energy ion beams has been performed and reported by Biryukov and Bellucci [6]. Theoretical modeling of ion channeling in MeV energy range through carbon nanotubes (where dynamic polarization of nanotube electrons play an important role) has been also studied [17,18,21]. Krasheninnkov and Nordlund [8] have been investigated channeling of low energy Ar^+ ions through carbon nanotubes.

While theoretical approach reached a mature level, the experimental advancement in this area is still in its infancy. The most challenging task in such experiments still is to solve the problems of ordering, straightening and holding nanotubes. Experimental evidence of ion channeling through carbon nanotubes has been reported by Zhu et al. [30]. They successfully measured channeling of He^+ ions of the energy of 2 MeV through carbon nanotubes. The first experimental results on electron channeling through carbon nanotubes has been reported by Chai et al. [31]. They studied the transport of electrons of the energy of 300 keV through the well aligned MWNTs. The lengths of nanotubes was 0.7–3.0 μm and misalignment of the nanotubes was up to 1°.

If we apply external mechanical stress on carbon nanotube, radial deformation can appear [32,33]. Also, carbon nanotube can be radially deformed if we apply external electric field [34,35] or if we use atomic force microscope [34]. Radial deformation of carbon nanotubes can influence on the mechanical and electronic properties [32–35], and presence of defects and deformations might have

large influence of nanotube's channeling properties. The channeling potential in deformed SWNTs has been investigated by Abu-Assy and Saliman [36].

This work is continuation of our previous investigation [37]. In the present work we have presented a theoretical investigation of the channeling of high energy protons with the radial deformed (10, 0)@(5, 0) DWNTs. Proton energy is varied from 0.1 to 10 GeV. For the first time we presented theoretically obtained spatial and angular distributions of channeled protons with radially deformed DWNTs.

We organized paper in the following way. In Section 2 we explained the process of ion channeling in carbon nanotubes. In Section 3 we presented and discussed channeling potential of radial deformed DWNT. Also, we obtained and presented the spatial and angular distributions of protons channeling through radial deformed DWNTs. The concluding remarks are given in Section 4.

2. Theory

Nanotubes can be the single-wall (SW), double-wall (DW) or multi-wall (MW) ones, depending on the number of cylinders they include. In this paper we consider the DWNTs as a straight coaxial cylinders with a circular or elliptical cross-section, depending on whether the radial deformation does not exist or exist, respectively (see Figure 1).

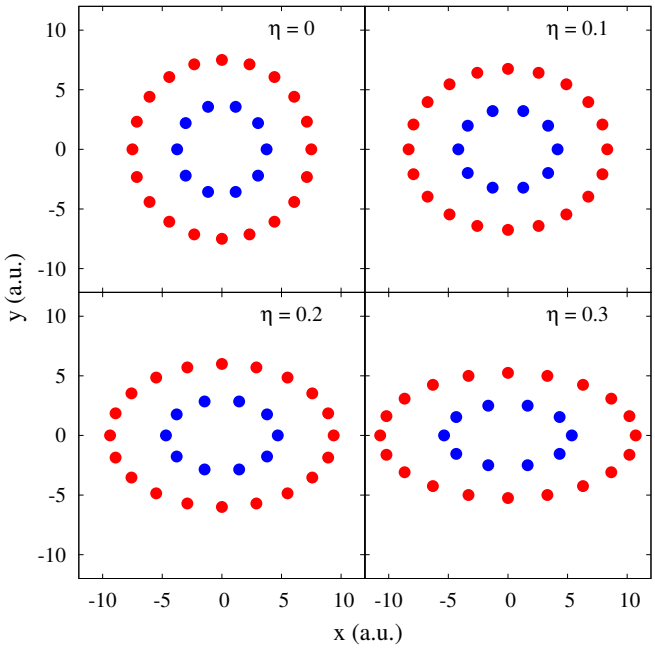

Figure 1. The view along axes of short DWNTs(10, 0)@(5, 0) under different radial strains: (left top) $\eta = 0$ (perfect nanotube); (right top) $\eta = 0.1$; (left down) $\eta = 0.2$; (right down) $\eta = 0.3$, respectively.

We used classical approach to consider interaction of the proton and a carbon nanotube atoms. Reasons are the following: A 0.1 GeV energy proton has a velocity of $v = 58.8619$ a.u. ($c = 137.0355$ a.u.), a rest mass of $m_0 = 1822.9$ a.u., a relativistic mass of $m_r = 2018.61$ a.u. and a wavelength $\lambda = 2.7983 \times 10^{(-6)}$ nm. A 1 GeV energy proton has a velocity of $v = 120.0474$ a.u., a relativistic mass of $m_r = 3779.97$ a.u. and a wavelength $\lambda = 7.3271 \times 10^{(-7)}$ nm. In both cases lambda is much smaller than the bond length between nanotube atoms (0.144 nm) [38]. For higher energies wavelength λ is even smaller. That is why we treat this problem classically. Also, it is shown that transverse motion of protons can be treated classically [6,28] even for lower energies than energy considered in our paper. Even in case of light particles, e.g., electron (positron) energies about 10 MeV it becomes possible to use classical mechanics [10] because the number of transverse states in the axial potential wells grows approximately linearly with the particle energy E [10]. Very similar analysis of motion of charged particles are considered [4,39], but in the case of charged particles of much

lower energies quantum approach should be applied [10,25,29]. We want to stress that in case of proton channeling through Si crystal, using very similar theoretical model and classical approach (3.2 MeV protons) with Moliere continuum potential approximation we get very nice agreement between theoretical calculation and experiment (see Figures 3 and 4 from reference [40]). Also, theoretical predictions from Figure 1 from reference [40], case of 10 MeV protons give nice agreement with later experiments [41–43].

We adopt the right Cartesian coordinate system with the z axis coinciding with the nanotube axis, where the origin lies in the entrance plane of the nanotube, and the x and y axes are the horizontal and vertical axes, respectively. Proton initial velocity is along $-z$ direction. The lengths of the nanotubes, L, are in the range of few μm, i.e., large enough to allow us to ignore the influence of the nanotube edges and, at the same time, small enough to neglect the energy losses of channeled protons. We can neglect dynamic polarization effects of carbon nanotube valence electrons [13,14].

For energy range investigated in this paper (>0.1 GeV) dynamic polarization of valence electrons in the nanotubes can be omitted. For keV energies protons strong dynamic polarization of valence electrons in the nanotubes should be taken into account. This effect can give rise to a strong image force on the protons, as well as a considerable energy loss due to the collective, or plasma, electron excitations [13,14,18,44].

The proton equations of motion that we are solving are the following:

$$m_r \frac{d^2x(t)}{dt^2} = -\frac{\partial U(x,y)}{\partial x}, \quad x(0) = x_0, \ \frac{dx(t)}{dt}\Big|_{t=0} = 0 \tag{1}$$

$$m_r \frac{d^2y(t)}{dt^2} = -\frac{\partial U(x,y)}{\partial y}, \quad y(0) = y_0, \ \frac{dy(t)}{dt}\Big|_{t=0} = 0, \tag{2}$$

where $m_r = m_0/\sqrt{1-(v/c)^2}$ is the relativistic proton mass and m_0 is its rest mass, v is the intensity of the velocity vector of the proton and c is the speed of light.

The continuum model approximation is assumed [45]. The proton nanotube interaction potential $U(x,y)$ as a function of the proton-atom distance r can be expressed through the Molière's approximation of the Thomas-Fermi interaction potential [46] $V(r)$ in the following form:

$$U(x,y) = \sum_{k=1}^{J} \frac{1}{d} \int_{-\infty}^{\infty} V\left(\sqrt{\rho_k^2 + z^2}\right) dz, \tag{3}$$

where the k-th term in the sum represents the continuum interaction potential of the proton and the k-th atomic string, with the distance d between average centres of two adjacent carbon atoms along the row, while the ρ_k is the distance between the proton and k-th string. The total number of atomic strings in the nanotube is indicated by J. In our case of DWNTs(10, 0)@(5, 0) J = 30 (see Figure 1).

The spatial and angular distributions of transmitted protons are generated using a Monte Carlo computer simulation code. The components of the proton impact parameter, x_0 and y_0, are chosen randomly from a uniform distribution within the cross-sectional area of the nanotube and its entrance plane. The angle of the velocity vector of a proton with respect to the channel axis is relatively small and it remains small during proton channeling through the entire length of the nanotube [10], smaller than the critical angle for channeling. Channeled protons do not approach nanotube walls at distances which are shorter than the screening radius a_{sc} of the C atoms, because if a proton approaches the nanotube wall at a distance smaller than a_{sc} we consider it to undergo hard collision with a carbon atom giving rise to a deflection angle larger than the critical angle for channeling. Such proton is considered as dechanneled and we no longer follow its trajectory in our simulation. In ion channeling experiments, the always present question is of ion beam divergence. Technically, it is not problem to obtain low ion beam divergence well below 1° [42,43]. In this paper we investigate only ideal proton beam divergence of 0°. In our previous work of proton channeling with straight, ideal SWNT we also studied case when the initial proton velocity is not parallel to the nanotube axis. We show that,

as the proton incident angle increases and approaches the critical angle for channeling, a ring-like structure is developed in the angular distribution - donut effect [21,24]. Probably, the same situation will occur in case of DWNT and MWNT. Because it is much easier to produce straight and well aligned nanocapillary than nanotube, there are a lot of experimental and theoretical researches of ion guiding with nanocapillary, see the following papers and references therein [47–49].

3. Results and Discussion

The results are presented for radially deformed nanotubes characterized by the parameter η. The radial deformation is obtained by squeezing the nanotube in the y direction and elongating in the x direction and it is characterized by a dimensionless parameter η: $\eta = (R - R_y)/R$, where R_y is semi-minor axis and R is the radius of underfomed nanotube [34]. The intersection of the nanotube with the transverse plane gives an ellipse with semi-major axis R_x and semi-minor axis R_y (see Figure 1). On the other hand, the semi-axis can be expressed as a function of the radius R of the underfomed nanotube and the parameter η in the form of $R_x = R(1-\eta)^{-1}$ and $R_y = R(1-\eta)$. It is obvious from Figure 1 that the radial cross section of the nanotube can take different forms in case of different degrees of radial deformation.

We study the relatively small radial deformation, i.e., three cases η = 0.1, 0.2 and 0.3. The radius of carbon nanotube R is determined by following equation:

$$R = l\sqrt{3}(2\pi)^{-1}\left(n^2 + nm + m^2\right)^{1/2}, \tag{4}$$

where the (n, m) represents chiral index and l represents interatomic length (the bond length between carbon atoms ≈0.144 nm).

The position of the carbon atom of the k-th atomic string in a plane perpendicular to the nanotube axis is determined by the angle:

$$\theta_k = \arctan\left(\frac{R_y}{R_x}\tan\left(2\pi(k-1)/N\right)\right), \tag{5}$$

relative to the semi-major axis and the distance from the center of the SWNT [36]:

$$R_k = \left(R_x^{-2} - \sin^2\theta_k\left(R_x^{-2} - R_y^{-2}\right)\right)^{-1/2}. \tag{6}$$

The interaction potential can be represented in the following form:

$$U(x,y) = \frac{4Z_1Z_2e^2}{d} \times \sum_{k=1}^{N}\sum_{j=1}^{3} a_j K_0\left(b_j\sqrt{x^2 + y^2 + R_k^2 - 2\sqrt{x^2+y^2}R_k\cos\theta_k}\right), \tag{7}$$

where Z_1 = 1 and Z_2 = 6 are the atomic numbers of the proton and carbon atom, respectively, e is the elementary charge, $a_1 = 0.35$, $a_2 = 0.55$, $a_3 = 0.1$, $b_1 = 0.3/a_{tf}$, $b_2 = 1.2/a_{tf}$, $b_3 = 6/a_{tf}$, where $a_{tf} = (9\pi^2/(128Z_2))^{1/3}a_0$ is the screening Thomas-Fermi radius and a_0 is Bohr radius.

In case of our study DWNT(10, 0)@(5, 0) consists of SWNT(10, 0) and SWNT(5, 0). In Equation (4) we put n = 10, m = 0 for SWNT(10, 0), and n = 5, m = 0 for SWNT(5, 0) in order to get radii R of both nanotubes $R_{SWNT(10,\,0)}$ and $R_{SWNT(5,\,0)}$, respectively. In Equation (5) we put number of atomic strings N = 20 for SWNT(10, 0), and N = 10 for SWNT(5, 0) (see Figure 1), in order to get θ_k of both nanotubes, i.e., $\theta_{k,SWNT(10,\,0)}$ and $\theta_{k,SWNT(5,\,0)}$. Using Equations (4)–(7) we can calculate the interaction potential of SWNT(10, 0) and SWNT(5, 0), i.e., $U(x,y)_{SWNT(10,\,0)}$ and $U(x,y)_{SWNT(5,\,0)}$. Interaction potential of DWNTs(10, 0)@(5, 0) is obtained using following relation:

$$U(x,y)_{DWNT(10,\,0)@(5,\,0)} = U(x,y)_{SWNT(10,\,0)} + U(x,y)_{SWNT(5,\,0)}. \tag{8}$$

Figure 1 presents the view along axes of short DWNTs(10, 0)@(5, 0) for perfect nanotube (η = 0) and under three different radial strains: η = 0.1, 0.2 and 0.3. It is presented positions of atomic strings for DWNTs(10, 0)@(5, 0), which consists of inner nanotube (5, 0) (10 atomic strings) and outer nanotube (10, 0) (20 atomic strings) in all 4 cases.

We will first analyze the contour plot of the channeling potential $U(x, y)$ in the xy plane of DWNTs(10, 0)@(5, 0) with perfect straight nanotube and with nanotube under radial strains. After that we will present and discuss corresponding spatial and angular distributions for different proton initial energies E and for different nanotube lengths L.

Figure 2 shows contour plots of the channeling potential $U(x, y)$ in the xy plane of DWNTs(10, 0)@(5, 0) for perfect nanotube and for nanotubes under three different radial strains. The case η = 0 represents perfect straight nanotube. The potential is changing very quickly near the nanotube wall i.e., close to atomic rows and the changing of potential is very slowly near the nanotube center. The minimum value of potential is at the nanotube center. As the value of radial deformation strain increases the contour plot of channeling potential get more elliptical shape (with increase of ellipse eccentricity). We can conclude that there is high influence of values of radial strains on the nanotube channeling potential.

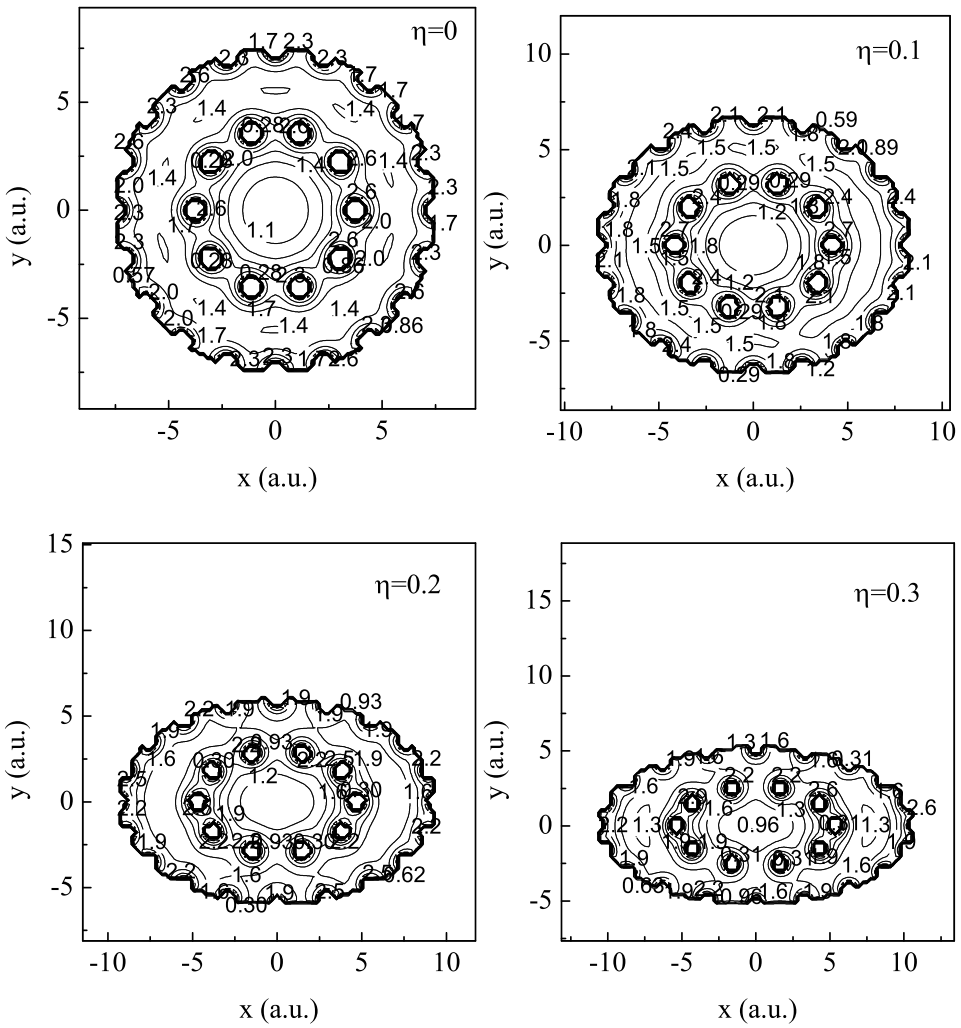

Figure 2. Contour plot of the channeling potential $U(x, y)$ in the xy plane of DWNTs(10, 0)@(5, 0) under different radial strains: (left top) η = 0; (right top) η = 0.1; (left down) η = 0.2; (right down) η = 0.3, respectively.

Figure 3 presents spatial distributions of the $E = 1$ GeV protons channeled in the radially deformed DWNTs(10, 0)@(5, 0) under different radial strains: $\eta = 0$, 0.1, 0.2 and 0.3. The nanotube length is $L = 1$ μm. The areas with higher proton yield are designated by darker shading. We can notice that the under higher radial strains spatial distributions obtain the elliptical shape with increase of ellipse eccentricity. We can spot 20 maxima of proton yield lying in-between the atomic rows in the peripheral region and 10 maxima in the middle region of spatial distributions. These 10 maxima connect central structure in the spatial distribution with peripheral structure. The appearance of the 20 maxima is connected to the symmetry of the transverse geometrical structure of the nanotube, which consists of 20 atomic strings in the peripheral region (due to the outer nanotube) and 10 maxima in the middle region (due to the inner nanotube).

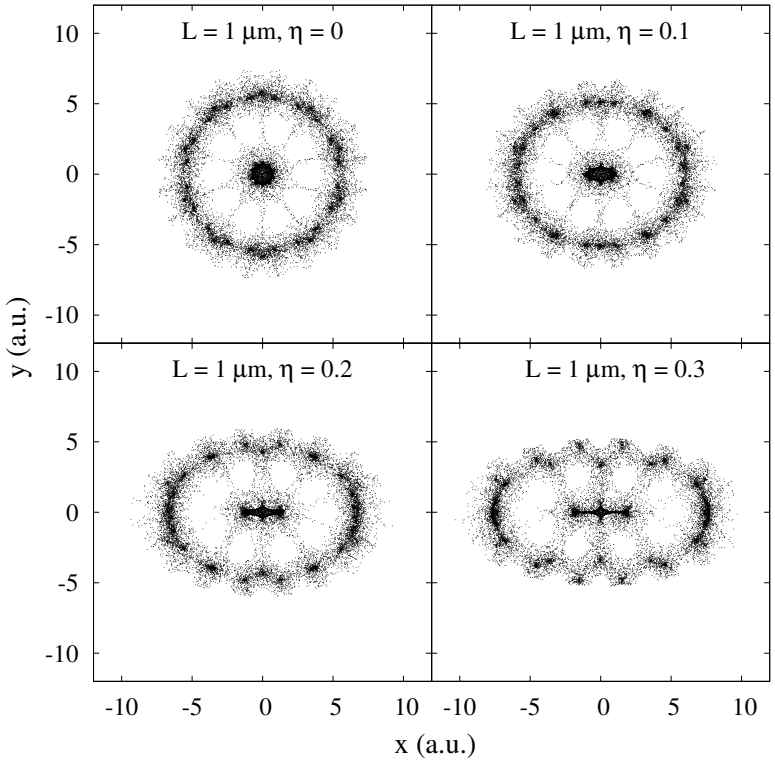

Figure 3. The spatial distributions of protons channeled in the radially deformed DWNTs(10, 0)@(5, 0) under different radial strains: (left top) $\eta = 0$; (right top) $\eta = 0.1$; (left down) $\eta = 0.2$; (right down) $\eta = 0.3$, respectively. The proton energy is $E = 1$ GeV and nanotube length is $L = 1$ μm.

Figure 4 shows angular distributions which correspond to spatial distributions presented in Figure 3. These are the cases of protons channeled in the radially deformed DWNTs(10, 0)@(5, 0) under different radial strains: $\eta = 0$, 0.1, 0.2 and 0.3. In the corresponding angular distributions, 10 maxima in the very peripheral region are pronounced. These maxima are due to inner nanotube. We can notice that the transverse geometrical structure of the nanotube is deducible from the angular distribution only in case of smaller radial strains: $\eta = 0$ and 0.1.

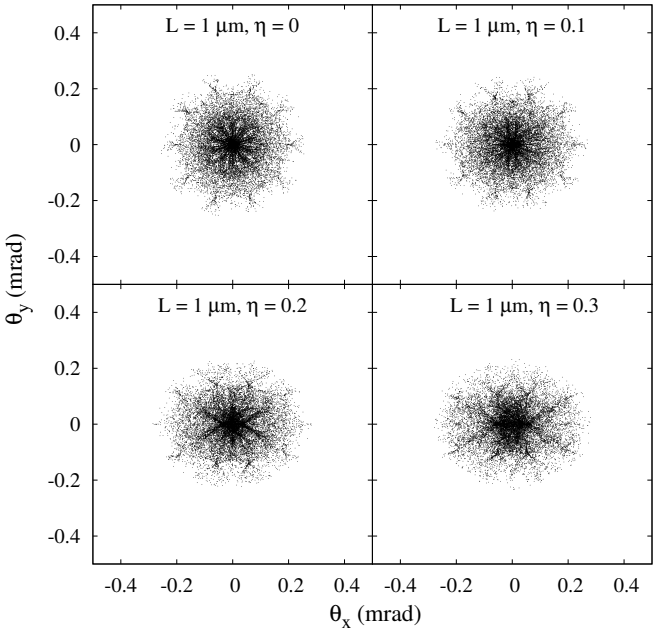

Figure 4. The angular distributions of protons channeled in the radially deformed DWNTs(10, 0)@(5, 0) under different radial strains: (left top) $\eta = 0$; (right top) $\eta = 0.1$; (left down) $\eta = 0.2$; (right down) $\eta = 0.3$, respectively. The proton energy is $E = 1$ GeV and nanotube length is $L = 1$ μm.

Figure 5 presents spatial distributions of the protons channeled in the radially deformed DWNTs(10, 0)@(5, 0) under different radial strains: $\eta = 0$, 0.1, 0.2 and 0.3 for proton energy $E = 1$ GeV and nanotube length $L = 3$ μm. We can see that increasing the length of nanotube from $L = 1$ to 3 μm (Figure 3) influenced strongly the shape of spatial distributions. Also, under different radial strains we obtain a significant redistribution of the proton flux within the nanotubes.

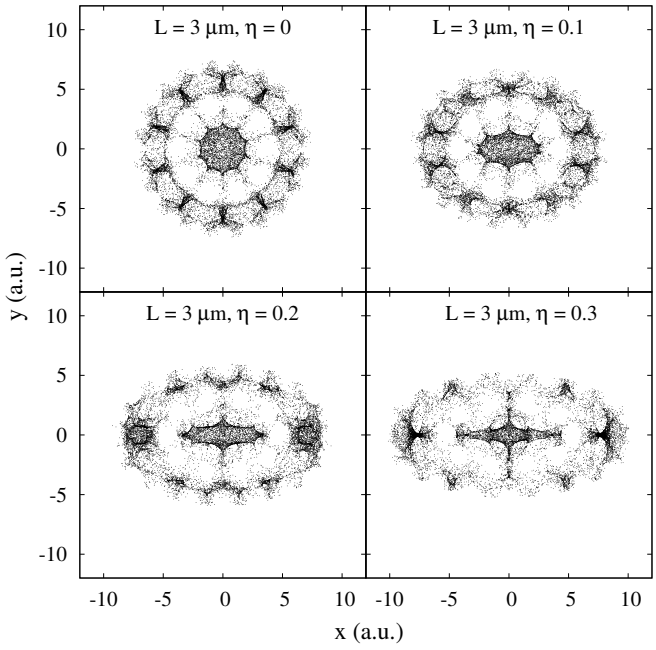

Figure 5. The spatial distributions of protons channeled in the radially deformed DWNTs(10, 0)@(5, 0) under different radial strains: (left top) $\eta = 0$; (right top) $\eta = 0.1$; (left down) $\eta = 0.2$; (right down) $\eta = 0.3$, respectively. The proton energy is $E = 1$ GeV and nanotube length is $L = 3$ μm.

Figure 6 shows angular distributions of the protons channeled in the radially deformed DWNTs(10, 0)@(5, 0) under different radial strains: η = 0, 0.1, 0.2 and 0.3. The proton energy is E = 1 GeV and nanotube length is L = 3 μm. These angular distributions correspond to spatial distributions presented in Figure 5. The angular distributions are characterized by 10 maxima in the very peripheral region. We can notice that the transverse geometrical structure of the nanotube is very hard deducible from the angular distributions, much harder than in the case L = 1 μm.

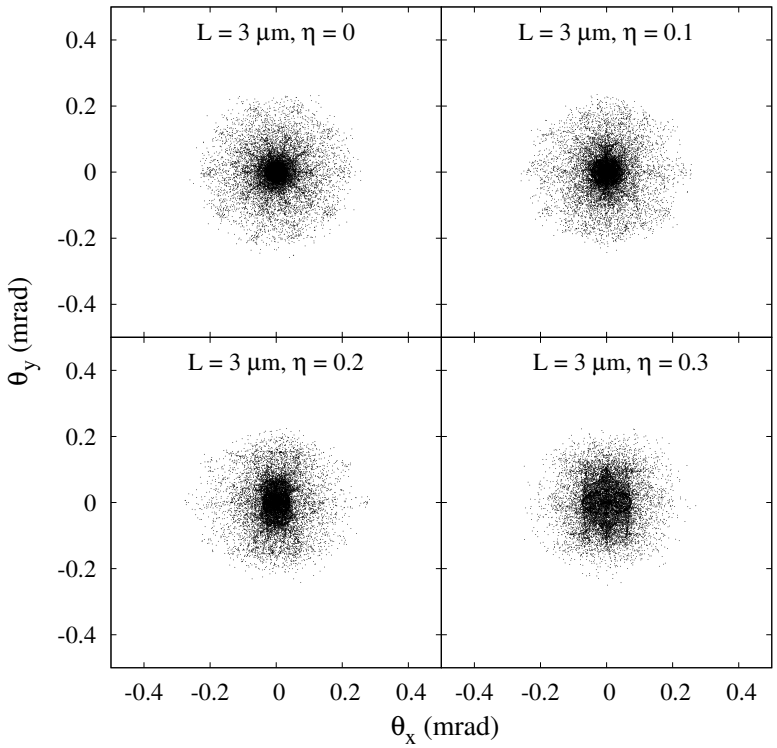

Figure 6. The angular distributions of protons channeled in the radially deformed DWNTs(10, 0)@(5, 0) under different radial strains: (left top) η = 0; (right top) η = 0.1; (left down) η = 0.2; (right down) η = 0.3, respectively. The proton energy is E = 1 GeV and nanotube length is L = 3 μm.

Figure 7 presents the spatial distributions of protons channeled in the radially deformed DWNTs(10, 0)@(5, 0) for different proton energies: E = 0.1, 0.5, 2 and 10 GeV. We performed calculation for radial strain η = 0.1 and for nanotube length L = 1 μm. We fixed radial strain and length of nanotube and vary initial proton energy. We can see that the spatial distribution of protons within the nanotube is very dependent of initial proton energy. If the proton initial energy is higher, proton dwell time in nanotube is shorter and spatial distribution is less smeared out.

Figure 8 presents the angular distributions of protons channeled in the radially deformed DWNTs(10, 0)@(5, 0) for different proton energies: E = 0.1, 0.5, 2 and 10 GeV, the radial strain is η = 0.1 and the nanotube length is L = 1 μm. These angular distributions correspond to spatial distributions presented in Figure 7. We can notice that the shapes and dimensions of obtained angular distribution are very dependent on initial proton energy. If the proton initial energy is higher, dimension of angular distribution is smaller.

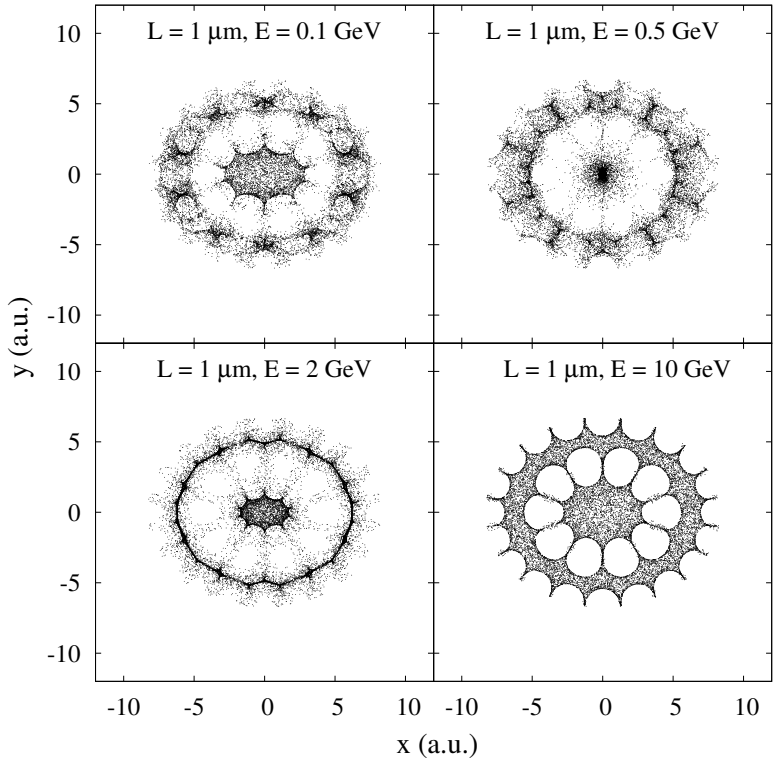

Figure 7. The spatial distributions of protons channeled in the radially deformed DWNTs(10, 0)@(5, 0) for different proton energies: (left top) E = 0.1 GeV; (right top) E = 0.5 GeV; (left down) E = 2 GeV; (right down) E = 10 GeV, respectively. The radial strain is η = 0.1 and nanotube length is L = 1 μm.

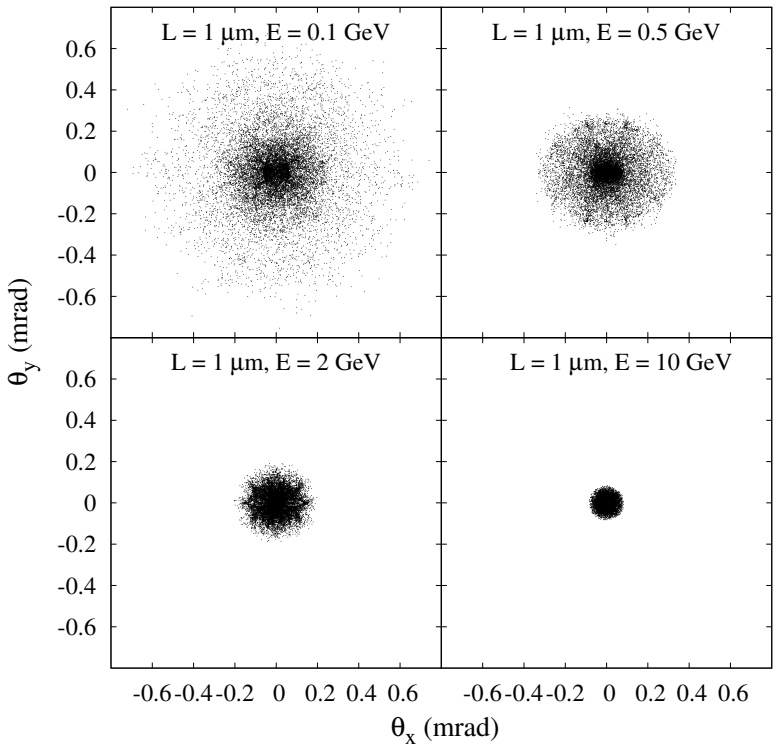

Figure 8. The angular distributions of protons channeled in the radially deformed DWNTs(10, 0)@(5, 0) for different proton energies: (left top) E = 0.1 GeV; (right top) E = 0.5 GeV; (left down) E = 2 GeV; (right down) E = 10 GeV, respectively. The radial strain is η = 0.1 and nanotube length is L = 1 μm.

Figure 9 presents the spatial distributions of protons channeled in the radially deformed DWNTs(10, 0)@(5, 0) for different nanotube lengths: L = 1, 3, 5 and L = 7 μm. The radial strain is η = 0.1 and the proton incidence energy is E = 10 GeV. We fixed radial strain of nanotube and proton initial energy and vary nanotube length. It can be seen that the obtained spatial distributions are very dependent on nanotube lengths.

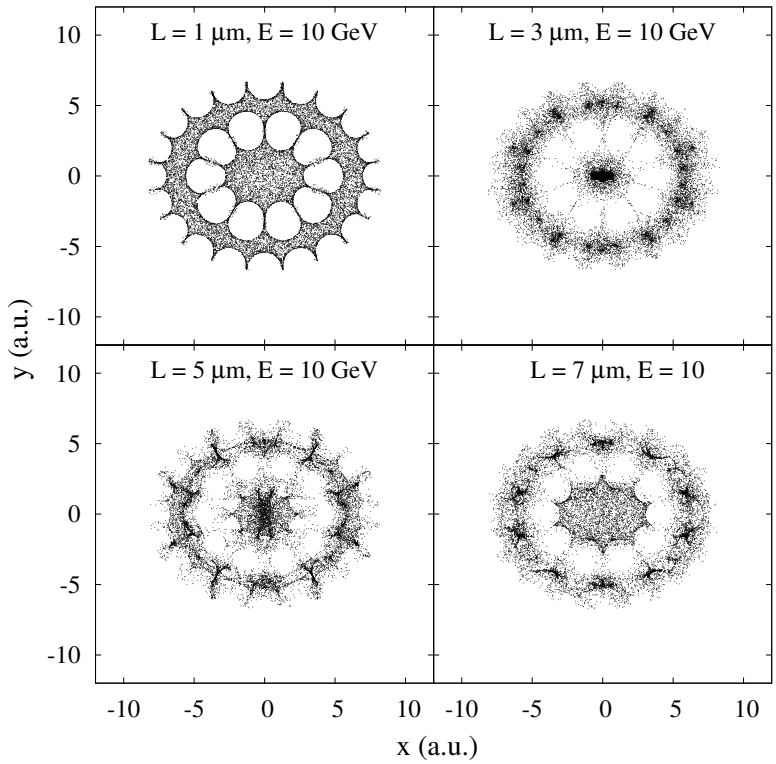

Figure 9. The spatial distributions of protons channeled in the radially deformed DWNTs(10, 0)@(5, 0) for different nanotube lengths: (left top) L = 1 μm; (right top) L = 3 μm; (left down) L = 5 μm; (right down) L = 7 μm, respectively. The radial strain is η = 0.1 and the proton energy is E = 1 GeV.

Figure 10 presents the angular distributions of protons channeled in the radially deformed DWNTs(10, 0)@(5, 0) for different nanotube lengths: L = 1, 3, 5 and L = 7 μm. The radial strain is η = 0.1 and the proton incidence energy is E = 10 GeV. It can be seen that if the nanotube length increase the angular and corresponding spatial distributions (see Figure 9) are more smeared out and it is harder to deduce transverse structure of the nanotube.

Like in previous investigation with SWNTs [37], we can conclude that the both, spatial and angular distributions are very sensitive to the value of radial strain and nanotube length. Also, they are very sensitive to the value of incidence proton energy [22]. These effect can be used to manipulate proton yields within the nanotube. The transverse geometrical structure of the nanotube is easier to deduce from the angular distribution in case of shorter nanotubes, smaller radial strains and higher incidence proton energy.

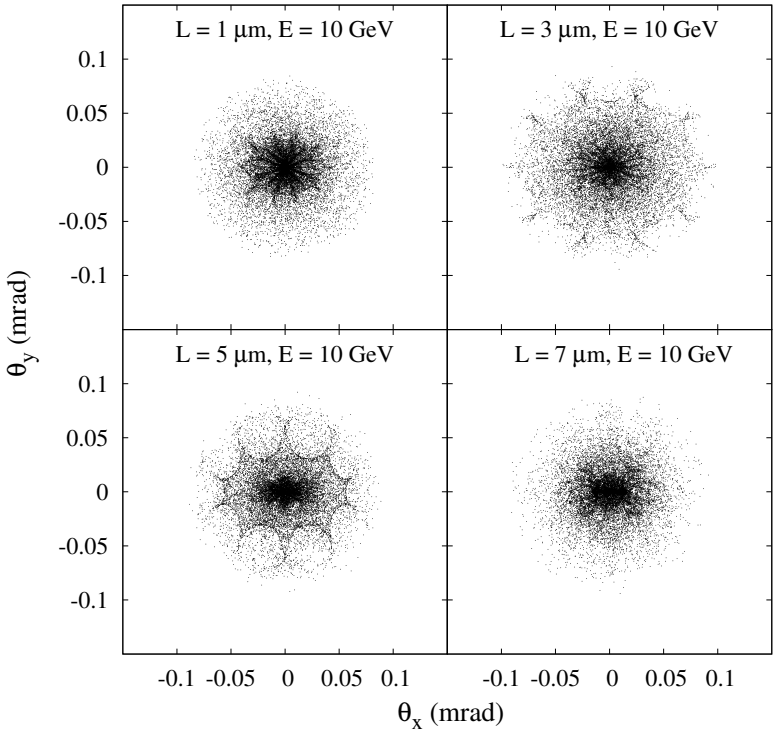

Figure 10. The angular distributions of protons channeled in the radially deformed DWNTs(10, 0)@(5, 0) for different nanotube lengths: (left top) L = 1 μm; (right top) L = 3 μm; (left down) L = 5 μm; (right down) L = 7 μm, respectively. The radial strain is η = 0.1 and the proton energy is E = 1 GeV.

4. Conclusions

Here, we have analyzed in theoretical manner the channeling of high energy protons through the radial deformed DWNTs(10, 0)@(5, 0). Proton energy is varied from 0.1 to 10 GeV and nanotube length L is varied from 1 to 7 μm. In our calculation we take into account the different degrees of radial deformation of the DWNTs, i.e., we performed calculation for perfect nanotube and under three different radial strains: η = 0.1, 0.2 and 0.3. We presented a contour plots of nanotube channeling potential. Also, for the first time we presented theoretically obtained spatial and angular distributions of channeled protons with radially deformed DWNTs. Monte Carlo simulation method was used to compute the spatial and angular distributions of channeled protons. The analysis has been done using the Molière's expression for the continuum potential of the nanotube atoms.

We showed that the spatial and angular distributions of channeled protons depend strongly on the radial strain, length of nanotube and the initial energy of channeled protons. We take into account the effect of the radial deformation because majority of nanotubes are radially deformed. We performed calculation for DWNTs, because experimental evidence of ion and electron channeling through carbon nanotubes has been reported with MWNTs [30,31], because it is harder to solve the problems of ordering, straightening and holding SWNTs than MWNTs. Also, the analysis shows that for short length of nanotubes and low value of radial deformation (η = 0.1) the transverse geometrical structure of the nanotubes can be deduced from the angular distribution (we can identify the type of nanotube, i.e., in case of DWNT we can determine inner and outer nanotube). We believe that detailed study of protons channeling through deformed DWNT may be useful to give us detailed information on the relevant interaction potentials inside nanotubes and for creating and guiding nanosized ion beams.

Author Contributions: The both coauthors participated in calculation and discussion of obtained results. The authors contributed equally to this work.

Acknowledgments: This work is supported by Ministry of Education, Science and Technological Development of the Republic of Serbia, through the project 45005.

Funding: This research received no external funding.

Conflicts of Interest: The authors declare no conflict of interest.

Abbreviations

The following abbreviations are used in this manuscript:

DWNT	Double-wall carbon nanotubes
MC	Monte Carlo
MWNT	Multi-wall carbon nanotubes
SWNT	Single-wall carbon nanotubes

References

1. Iijima, S. Helical microtubules of graphitic carbon. *Nature* **1991**, *354*, 56–58. [CrossRef]
2. Klimov, V.V.; Letokhov, V.S. Hard X-radiation emitted by a charged particle moving in a carbon nanotube. *Phys. Lett. A* **1996**, *222*, 424–428. [CrossRef]
3. Dedkov, G.V. Fullerene nanotubes can be used when transporting gamma-quanta, neutrons, ion beams and radiation from relativistic particles. *Nucl. Instrum. Meth. Phys. Res. B* **1998**, *143*, 584–590. [CrossRef]
4. Zhevago, N.K.; Glebov, V.I. Channeling of fast charged and neutral particles in nanotubes. *Phys. Lett. A* **1998**, *250*, 360–368. [CrossRef]
5. Gevorgian, L.A.; Ispirian, K.A.; Ispirian, R.K. High energy particle channeling in nanotubes. *Nucl. Instrum. Meth. Phys. Res. B* **1998**, *145*, 155–159. [CrossRef]
6. Biryukov, V.M.; Bellucci, S. Nanotube diameter optimal for channeling of high-energy particle beam. *Phys. Lett. B* **2002**, *542*, 111–115. [CrossRef]
7. Greenenko, A.A.; Shulga, N.F. Fast ion passing through straight and bent nanotubes. *Nucl. Instrum. Meth. Phys. Res. B* **2003**, *205*, 767–772. [CrossRef]
8. Krasheninnikov, A.V.; Nordlund, K. Multiwalled carbon nanotubes as apertures and conduits for energetic ions. *Phys. Rev. B* **2005**, *71*, 245408. [CrossRef]
9. Bellucci, S.; Biryukov, V.M.; Cordelli, A. Channeling of high-energy particles in a multi-wall nanotube. *Phys. Lett. B* **2005**, *608*, 53–58. [CrossRef]
10. Artru, X.; Fomin, S.P.; Shulga, N.F.; Ispirian, K.A.; Zhevago, N.K. Carbon nanotubes and fullerites in high-energy and X-ray physics. *Phys. Rep.* **2005**, *412*, 89–189. [CrossRef]
11. Petrović, S.; Borka, D.; Nešković, N. Rainbows in transmission of high energy protons through carbon nanotubes. *Eur. Phys. J. B* **2005**, *44*, 41–45.
12. Borka, D.; Petrović, S.; Nešković, N. Channeling star effect with bundles of carbon nanotubes. *Phys. Lett. A* **2006**, *354*, 457–461. [CrossRef]
13. Borka, D.; Petrović, S.; Nešković, N.; Mowbray, D.J.; Mišković, Z.L. Influence of the dynamical image potential on the rainbows in ion channeling through short carbon nanotubes. *Phys. Rev. A* **2006**, *73*, 062902. [CrossRef]
14. Borka, D.; Petrović, S.; Nešković, N.; Mowbray, D.J.; Mišković, Z.L. Influence of the dynamical polarization effect on the angular distributions of protons channeled in double-wall carbon nanotubes. *Nucl. Instrum. Meth. Phys. Res. B* **2007**, *256*, 131–136. [CrossRef]
15. Matyukhin, S.I.; Frolenkov, K.Y. Critical Parameters of Channeling in Nanotubes. *Tech. Phys. Lett.* **2007**, *33*, 58–61. [CrossRef]
16. Moura, C.S.; Amaral, L. Carbon nanotube ropes proposed as particle pipes. *Carbon* **2007**, *45*, 1802–1807. [CrossRef]
17. Mišković, Z.L. Ion Channeling through Carbon Nanotubes. *Radiat. Eff. Defect Solids* **2007**, *162*, 185–205. [CrossRef]

18. Borka, D.; Mowbray, D.J.; Mišković, Z.L.; Petrović, S.; Nešković, N. Dynamic polarization effects on the angular distributions of protons channeled through carbon nanotubes in dielectric media. *Phys. Rev. A* **2008**, *77*, 032903. [CrossRef]
19. Zheng, L.-P.; Zhu, Z.-Y.; Li, Y.; Zhu, D.-Z.; Xia, H.-H. Ion mass dependence for low energy channeling in single-wall nanotubes. *Nucl. Instrum. Meth. Phys. Res. B* **2008**, *266*, 849–852. [CrossRef]
20. Matyukhin, S.I. Efficiency of Ion Deviation by Bent Carbon Nanotubes. *Tech. Phys. Lett.* **2009**, *35*, 318–321. [CrossRef]
21. Borka, D.; Mowbray, D.J.; Mišković, Z.L.; Petrović, S.; Nešković, N. Donut and dynamic polarization effects in proton channeling through carbon nanotubes. *New J. Phys.* **2010**, *12*, 043021. [CrossRef]
22. Borka, D.; Petrović, S.; Nešković, N. Channeling of protons through carbon nanotubes. In *Nanotechnology Science and Technology*; Science Publishers: New York, NY, USA, 2011; pp. 1–78, ISBN 978-1-61122-050-6.
23. Borka, D.; Lukić, V.; Timko, J.; Borka Jovanović, V. Using proton beams as a diagnostic tool in carbon nanotubes. *Nucl. Instrum. Meth. Phys. Res. B* **2012**, *279*, 169–172. [CrossRef]
24. Borka, D.; Lukić, V.; Timko, J.; Borka Jovanović, V. Identification of the types of carbon nanotubes using donut effects. *Nucl. Instrum. Meth. Phys. Res. B* **2012**, *279*, 198–201. [CrossRef]
25. Aleksandrov, V.A.; Filippov, G.M. Study of the rearrangement of a hydrogen atom moving parallel to the carbon nanotube wall. *J. Surf. Investig. X-ray Synchrotron Neutron Tech.* **2012**, *6*, 338–342. [CrossRef]
26. Babaev, A.; Dabagov, S.B. Simulations of planar channeling of relativistic nuclei in a bent crystal. *Eur. Phys. J. Plus* **2012**, *127*, 62. [CrossRef]
27. Zhang, Y.-Y.; Sun, J.-Z.; Song, Y.-H.; Mišković, Z.L.; Wang, Y.-N. Channeling of protons in single-walled carbon nanotubes based on kinetic and molecular-dynamics treatment. *Carbon* **2014**, *71*, 196–205. [CrossRef]
28. Karabarbounis, A.; Sarros, S.; Trikalinos, C. Channeling of protons in various types of radially compressed carbon nanotubes. *Nucl. Instrum. Meth. Phys. Res. B* **2015**, *355*, 316–319. [CrossRef]
29. Ćosić, M.; Petrović, S.; Nešković, N. Quantum primary rainbows in transmission of positrons through very short carbon nanotubes. *Nucl. Instrum. Meth. Phys. Res. B* **2016**, *373*, 52–62. [CrossRef]
30. Zhu, Z.; Zhu, D.; Lu, R.; Xu, Z.; Zhang, W.; Xia, H. The experimental progress in studying of channeling of charged particles along nanostructure. In *Proceedings SPIE, Proceedings of the International Conference on Charged and Neutral Particles Channeling Phenomena, Rome, Italy, 2004*; SPIE: Bellingham, WA, USA, 2005; Volume 5974, pp. 1–13.
31. Chai, G.; Heinrich, H.; Chow, L.; Schenkel, T. Electron transport through single carbon nanotubes. *Appl. Phys. Lett.* **2007**, *91*, 103101. [CrossRef]
32. Hasegawa, M.; Nishidate, K. Radial deformation and stability of single-wall carbon nanotubes under hydrostatic pressure. *Phys. Rev. B* **2006**, *74*, 115401. [CrossRef]
33. Imtani, A.N.; Jindal, V.K. Structure of armchair single-wall carbon nanotubes under hydrostatic pressure. *Phys. Rev. B* **2007**, *76*, 195447. [CrossRef]
34. Shtogun, Y.V.; Woods, L.M. Electronic Structure Modulations of Radially Deformed Single Wall Carbon Nanotubes under Transverse External Electric Fields. *J. Phys. Chem. C* **2009**, *113*, 4792–4796. [CrossRef]
35. Kan, B.; Ding, J.; Yuan, N.; Wang, J.; Chen, Z.; Chen, X. Transverse electric field–induced deformation of armchair single-walled carbon nanotube. *Nanoscale Res. Lett.* **2010**, *5*, 1144–1149. [CrossRef] [PubMed]
36. Abu-Assy, M.K.; Soliman, M.S. Channeling potential in single-walled carbon nanotubes: The effect of radial deformation. *Nucl. Instrum. Meth. Phys. Res. B* **2016**, *384*, 93–99. [CrossRef]
37. Borka Jovanović, V.; Borka, D.; Galijaš, S.M.D. Channeling of protons through radial deformed carbon nanotubes. *Phys. Lett. A* **2017**, *381*, 1687–1692. [CrossRef]
38. Saito, R.; Dresselhaus, G.; Dresselhaus, M.S. *Physical Properties of Carbon Nanotubes*; Imperial College Press: London, UK, 2001.
39. Gemmell, D.S. Channeling and related effects in the motion of charged particles through crystals. *Rev. Mod. Phys.* **1974**, *46*, 129–236. [CrossRef]
40. Borka, D.; Petrović, S.; Nešković, N. Doughnuts with a <110> very thin Si crystal. *J. Electron. Spectrosc. Relat. Phenom.* **2013**, *129*, 183–187.
41. Dang, Z.Y.; Motapothula, M.; Ow, Y.S.; Venkatesan, T.; Breese, M.B.H.; Rana, M.A.; Osman, A. Fabrication of large-area ultra-thin single crystal silicon membranes. *Appl. Phys. Lett.* **2011**, *99*, 223105. [CrossRef]
42. Motapothula, M.; Dang, Z.Y.; Venkatesan, T.; Breese, M.B.H.; Rana, M.A.; Osman, A. Influence of the Narrow f111g Planes on Axial and Planar Ion Channeling. *Phys. Rev. Lett.* **2012**, *108*, 195502. [CrossRef]

43. Motapothula, M.; Dang, Z.Y.; Venkatesan, T.; Breese, M.B.H.; Rana, M.A.; Osman, A. Axial ion channeling patterns from ultra-thin silicon membranes. *Nucl. Instrum. Meth. Phys. Res. B* **2012**, *283*, 29–34. [CrossRef]
44. Karbunar, L.; Borka, D.; Radović, I. Image potential and stopping force in the interaction of fast ions with carbon nanotubes: The extended two-fluid hydrodynamic model. *Nucl. Instrum. Meth. Phys. Res. B* **2016**, *366*, 83–89. [CrossRef]
45. Lindhard, J.K. Influence of crystal lattice on motion of energetic charged particles. In *Matematisk-fysiske Meddelelserudgivet af Det Kongelige Danske Videnskabernes Selskab*; Munksgaard: Copenhagen, Denmark, 1965; Volume 34.
46. Molière, G. Theorie der Streuung schneller geladener Teilchen I: Einzelstreuung am abgeschirmten Coulomb-Feld. *Zeitschrift für Naturforschung A* **1947**, *2*, 133–145. [CrossRef]
47. Stolterfoht, N. Simulation and analysis of ion guiding through a nanocapillary in insulating polymers. *Phys. Rev. A* **2013**, *87*, 012902. [CrossRef]
48. Lemell, C.; Burgdorfer, J.; Aumayr, F. Interaction of charged particles with insulating capillary targets—The guiding effect. *Prog. Surf. Sci.* **2013**, *88*, 237–278. [CrossRef]
49. Stolterfoht, N.; Yamazaki, Y. Guiding of charged particles through capillaries in insulating materials. *Phys. Rep.* **2016**, *629*, 1–107. [CrossRef]